

# Spectroscopy in the Ultraviolet and Visible Regions As Studied by Solution-Phase and Vapor-Phase Photoabsorption in the Ultraviolet and Visible Regions<sup>†</sup>

Jennifer C. Green\*

*Inorganic Chemistry Laboratory, University of Oxford, South Parks Road,  
Oxford OX1 3QR, Great Britain*

Sergey Yu. Ketkov\*

*G. A. Razuvaev Institute of Organometallic Chemistry of the Russian Academy of Sciences,  
Tropinin St. 49, Nizhny Novgorod 603600, Russia*

Received February 27, 1996<sup>⊗</sup>

The electronic absorption spectra of  $(\eta^7\text{-C}_7\text{H}_7)(\eta^5\text{-C}_5\text{H}_5)\text{V}$  and  $(\eta^7\text{-C}_7\text{H}_7)(\eta^5\text{-C}_5\text{H}_4\text{Me})\text{Ta}$  in *n*-heptane solution and in the vapor phase have been measured. Assignments of absorption features in the solution-phase spectra have been suggested on the basis of evaluated energies of electronic excitations. The spectra of both complexes change dramatically on going from the solution to the vapor phase due to the appearance of intense Rydberg bands which have been assigned unambiguously on the basis of their term values. All of them originate at the metal-localized  $d(\sigma^+)$  orbital. The vapor-phase spectrum of  $(\eta^7\text{-C}_7\text{H}_7)(\eta^5\text{-C}_5\text{H}_5)\text{V}$  reveals the lowest Rydberg  $s(\sigma^+)$  and  $p(\sigma^+)$  excitations as well as two first members of the  $Rmp(\pi)$  series. These Rydberg excitations are observed also in the spectrum of gas-phase  $(\eta^7\text{-C}_7\text{H}_7)(\eta^5\text{-C}_5\text{H}_4\text{Me})\text{Ta}$ , which shows additionally two absorption bands arising from the lowest Rydberg  $d$  transitions. The first member of the  $Rnd$  series in  $(\eta^7\text{-C}_7\text{H}_7)(\eta^5\text{-C}_5\text{H}_5)\text{V}$  is broadened beyond detection due to an admixture of a valence shell excitation. The IE corresponding to the detachment of an electron promoted onto the vacant valence shell and Rydberg orbitals has been estimated. On this basis, an IE diagram of unoccupied orbitals including both intravalency and Rydberg levels has been constructed for the two compounds. The lowest vacant level in both complexes is composed mainly of the  $\delta(e_2'')$  orbital of the cycloheptatrienyl ring. The second empty level corresponds to the antibonding  $d(\pi)$  orbital in  $(\eta^7\text{-C}_7\text{H}_7)(\eta^5\text{-C}_5\text{H}_5)\text{V}$  and the lowest Rydberg  $s(\sigma^+)$  level in  $(\eta^7\text{-C}_7\text{H}_7)(\eta^5\text{-C}_5\text{H}_4\text{Me})\text{Ta}$ . The diagram shows that the role of Rydberg orbitals should be taken into consideration when dealing with the vapor-phase physical and chemical processes involving low-lying vacant levels of transition-metal  $(\eta^7\text{-cycloheptatrienyl})(\eta^5\text{-cyclopentadienyl})$  derivatives.

## Introduction

The chemistry of transition-metal  $\eta^7$ -cycloheptatrienyl derivatives has been intensively developed during the last two decades,<sup>1</sup> attracting growing attention to the electronic structure of such compounds. Within this class of organometallics, the mixed sandwich complexes with a  $\eta^5$ -cyclopentadienyl ring as the second ligand are of particular interest since they represent the most convenient model compounds for understanding of the bonding between transition metals and the cycloheptatrienyl moiety.<sup>2–9</sup>

To study the electronic structures of the  $(\text{Ch})(\text{Cp})\text{M}$  systems ( $\text{Ch} = \eta^7\text{-C}_7\text{H}_7$ ,  $\text{Cp} = \eta^5\text{-C}_5\text{H}_5$ ), both theoretical<sup>2–4</sup> and experimental<sup>5–11</sup> methods have been employed and an interaction scheme has been established for the metal and ligand levels. A qualitative molecular orbital (MO) diagram is given in Figure 1. The  $d$  and  $\text{Cp}$  or  $\text{Ch}$  labels in the designation of MOs on this diagram reflect the predominant contribution of the metal and ligand orbitals, respectively.

The X-ray crystal structures of  $(\text{Ch})(\text{Cp})\text{M}$  ( $\text{M} = \text{Ti},^{12} \text{V},^{13} \text{Cr}^{14}$ ) and the molecular structure of  $(\text{Ch})(\text{Cp})\text{Nb}$  studied by electron diffraction<sup>15</sup> show that the carbon atoms of the two ligands lie in parallel planes. Mixed

<sup>†</sup> This paper is dedicated to Professor G. A. Domrachev on the occasion of his 60th birthday.

<sup>⊗</sup> Abstract published in *Advance ACS Abstracts*, September 15, 1996.

- (1) Green, M. L. H.; Ng, D. K. P. *Chem. Rev.* **1995**, *95*, 439.
- (2) Warren, K. D. *Struct. Bonding* **1976**, *27*, 45.
- (3) Clack, D. W.; Warren, K. D. *Theor. Chim. Acta* **1977**, *46*, 313.
- (4) Zeinstra, J. D.; Nieuwpoort, W. C. *Inorg. Chim. Acta* **1978**, *30*, 103.
- (5) Evans, S.; Green, J. C.; Jackson, S. E.; Higginson, B. *J. Chem. Soc., Dalton Trans.* **1974**, 304.
- (6) Groenenboom, C. J.; De Liefde Meijer, H. J.; Jellinek, F.; Oskam, A. *J. Organomet. Chem.* **1975**, *97*, 73.
- (7) Davies, C. E.; Gardiner, I. M.; Green, J. C.; Green, M. L. H.; Hazel, N. J.; Grebenik, P. D.; Mtetwa, V. S. B.; Prout, K. *J. Chem. Soc., Dalton Trans.* **1985**, 669.

(8) Green, J. C.; Green, M. L. H.; Kaltsoyannis, N.; Mountford, P.; Scott, P.; Simpson, S. *J. Organometallics* **1992**, *11*, 3353.

(9) Green, J. C.; Kaltsoyannis, N.; Sze, K. H.; MacDonald, M. *J. Am. Chem. Soc.* **1994**, *116*, 1994.

(10) Elschenbroich, Ch.; Gerson, F.; Stohler, F. *J. Am. Chem. Soc.* **1973**, *95*, 6956.

(11) Elschenbroich, Ch.; Bilger, E.; Metz, B. *Organometallics* **1991**, *10*, 2823.

(12) Zeinstra, J. D.; de Boer, J. L. *J. Organomet. Chem.* **1973**, *54*, 207.

(13) Engebreston, G.; Rundle, K. E. *J. Am. Chem. Soc.* **1963**, *85*, 481.

(14) Groenenboom, C. J.; De Liefde Meijer, H. J.; Jellinek, F. *J. Organomet. Chem.* **1974**, *69*, 235.

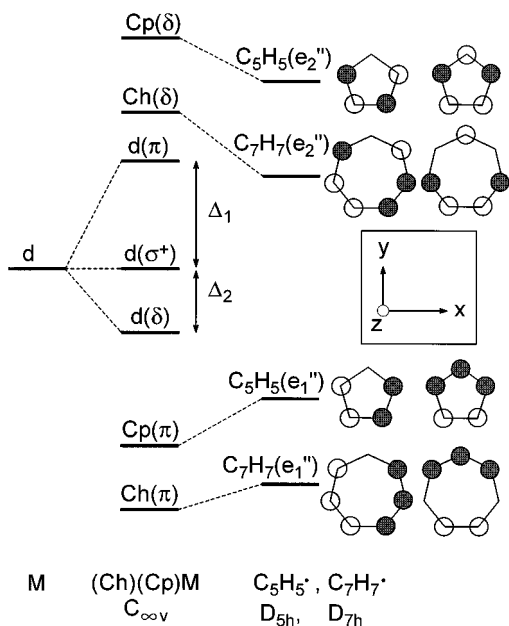


**Figure 1.** Qualitative molecular orbital diagram for (Ch)(Cp)M, with symmetry labels appropriate to the  $C_{\infty v}$  point group. The irreducible representations of the  $D_{7h}$  and  $D_{5h}$  point groups are used here to label the orbitals of the cycloheptatrienyl and cyclopentadienyl radicals, respectively. Shadings indicate the phases of the carbon  $2p_z$  atomic orbitals. The orbital separations comparable to the ligand field splittings  $\Delta_1$  and  $\Delta_2$  are shown.

sandwich compounds with planar carbocyclic rings are usually considered under the  $C_{\infty v}$  point group,<sup>2</sup> which gives three sets of metal d orbitals,  $d_z^2$  ( $\sigma^+$ ),  $d_{xz}$ ,  $d_{yz}$  ( $\pi$ ), and  $d_{x^2-y^2}$ ,  $d_{xy}$  ( $\delta$ ). The  $d_{xz}$ ,  $d_{yz}$ ,  $C_5H_5(e_1'')$  and  $d_{x^2-y^2}$ ,  $d_{xy}$ ,  $C_7H_7(e_2'')$  interactions, which result in formation of the  $Cp(\pi)$ ,  $d(\delta)$ ,  $d(\pi)$ , and  $Ch(\delta)$  levels in the sandwich complex (Figure 1), are mainly responsible for the metal–ligand bonding while the  $d(\sigma^+)$  orbital remains almost purely metallic in the (Ch)(Cp)M molecule.<sup>2–11</sup> As with the isoelectronic bisarene compounds, the ( $\eta^7$ -cycloheptatrienyl)( $\eta^5$ -cyclopentadienyl) derivatives of the group IV–VI transition metals can be described as 16-, 17-, and 18-electron complexes, respectively.<sup>16</sup> The order of the higher-lying occupied MOs in such systems has been well established on the basis of calculations<sup>2–4</sup> and photoelectron (PE) studies.<sup>5–9</sup> The nondegenerate  $d(\sigma^+)$  MO is the highest occupied orbital in 17- and 18-electron compounds. The  $d(\delta)$ ,  $Cp(\pi)$ , and  $Ch(\pi)$  orbitals lie deeper, as shown in Figure 1, the  $d(\delta)$  level representing the highest filled MO in the 16-electron (Ch)(Cp)M systems.

Information on unoccupied MOs of (Ch)(Cp)M is however much more limited. The nature, order, and symmetry of the excited states of polyatomic molecules can be determined by photoabsorption spectroscopy. Few studies have been made of electronic absorption spectra of these compounds. The solution-phase spectrum of (Ch)(Cp)V was studied by Gulick and Geske<sup>17</sup> thirty years ago, but no assignment was made. Some photoabsorption data for (Ch)(Cp)Ti have appeared in

more recent studies<sup>18,19</sup> without any suggestions on the nature of the intense bands. In our previous work,<sup>20,21</sup> the spectra of 18-electron sandwiches (Ch)(Cp)Cr and (Ch)(Cp)W were measured in the vapor and solution phases. In these studies, the attention was paid to the interpretation of the vapor-phase spectra which reveal clearly defined Rydberg bands.

Rydberg MOs of polyatomic molecules are formed by atomic orbitals (AOs) with a principal quantum number greater than that of the AOs contributing to the molecular valence shell. The smaller the energy required to detach an electron from an occupied MO, the smaller are the frequencies corresponding to the Rydberg transitions originating from this MO.<sup>22</sup> Rydberg levels were not taken into consideration when the qualitative MO diagram (Figure 1) was being constructed though they certainly should be present among the (Ch)(Cp)M lower-lying vacant orbitals because of the very low ionization energy (IE) corresponding to the occupied d levels.<sup>5–9</sup> Rydberg excitations have been shown to play an important role in the vapor-phase spectra of transition metal metallocenes,<sup>23,24</sup> bisarene complexes,<sup>25–27</sup> and mixed ( $\eta^6$ -arene)( $\eta^5$ -cyclopentadienyl) derivatives.<sup>28,29</sup> All Rydberg transitions observed originate from the nonbonding  $d(\sigma^+)$  orbital. Being well-resolved in the vapor phase, Rydberg bands disappear on going to condensed phases, so the spectra of gas-phase transition-metal sandwich compounds studied earlier<sup>20,21,23–29</sup> differed significantly from those recorded in organic solvents.

In our recent work,<sup>30</sup> possible assignments of absorption bands in the solution-phase spectrum of (Ch)(Cp)-Nb were given together with an interpretation of the Rydberg structure in the gas-phase photoabsorption spectrum. However, no attempt was made to arrange low-lying valence shell MOs and Rydberg orbitals in one and the same energetic scale. Described here is an investigation of the electronic absorption spectra of (Ch)(Cp)V and (Ch)(Cp')Ta ( $Cp' = \eta^5$ - $C_5H_4Me$ ) in the solution and vapor phases, which was undertaken to complete the series of photoabsorption studies of the group V transition metal ( $\eta^7$ -cycloheptatrienyl)( $\eta^5$ -cyclopentadienyl) derivatives and to construct a diagram of vacant MOs in the (Ch)(Cp)M systems including both valence shell and Rydberg levels. It would be especially interesting to reveal Rydberg bands in the vapor-phase spectrum of recently synthesized (Ch)(Cp')Ta since there has been no examples of Rydberg transitions originating at the tantalum-localized orbitals in polyatomic molecules up to now.

(18) Gourier, D.; Samuel, E. *Inorg. Chem.* **1988**, *27*, 3018.

(19) Anderson, J. E.; Maher, E. T.; Kool, L. B. *Organometallics* **1991**, *10*, 1248.

(20) Ketkov, S. Yu. *J. Organomet. Chem.* **1992**, *429*, C38.

(21) Green, J. C.; Green, M. L. H.; Field, C. N.; Ng, D. K. P.; Ketkov, S. Yu. *J. Organomet. Chem.* **1995**, *501*, 107.

(22) Robin, M. B. *Higher Excited States of Polyatomic Molecules*; Academic Press: New York, 1974; Vol. 1.

(23) Ketkov, S. Yu., Domrachev, G. A. *Inorg. Chim. Acta* **1990**, *178*, 233.

(24) Ketkov, S. Yu., Domrachev, G. A. *J. Organomet. Chem.* **1991**, *420*, 67.

(25) Domrachev, G. A.; Ketkov, S. Yu.; Razuvaev, G. A. *J. Organomet. Chem.* **1987**, *328*, 341.

(26) Ketkov, S. Yu., Domrachev, G. A.; Razuvaev, G. A. *J. Mol. Struct.* **1989**, *195*, 175.

(27) Ketkov, S. Yu., Domrachev, G. A. *J. Organomet. Chem.* **1990**, *389*, 187.

(28) Ketkov, S. Yu. *Opt. Spectrosc.* **1992**, *72*, 595.

(29) Ketkov, S. Yu. *J. Organomet. Chem.* **1994**, *465*, 225.

(30) Ketkov, S. Yu. *Russ. Chem. Bull.* **1994**, *43*, 583.

(15) Mawhorter, R. J.; Rankin, D. W. H.; Robertson, H. E.; Green, M. L. H.; Scott, P. *Organometallics* **1994**, *13*, 2401.

(16) Green, J. C. *Struct. Bonding* **1981**, *43*, 37.

(17) Gulick, W. M.; Geske, D. H. *Inorg. Chem.* **1967**, *6*, 1320.

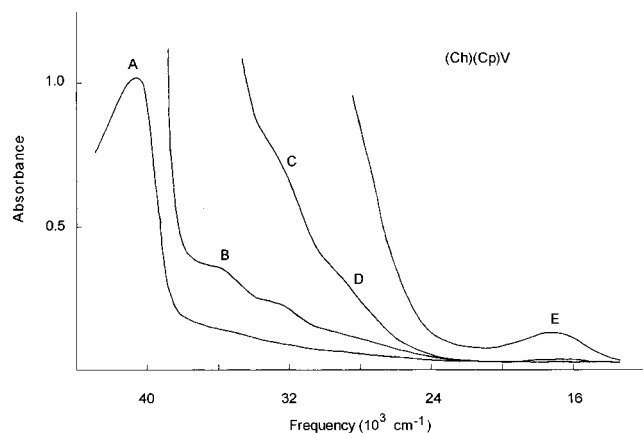


**Figure 2.** Electronic absorption spectrum of (Ch)(Cp)V in *n*-heptane solution. Concentrations for (Ch)(Cp)V were  $9 \times 10^{-5}$ ,  $3 \times 10^{-4}$ ,  $9 \times 10^{-4}$ , and  $6 \times 10^{-3}$  M.

### Experimental Section

(Ch)(Cp)V was synthesized by Dr. S. E. Jackson according to the literature procedure<sup>31</sup> and (Ch)(Cp')Ta was prepared by Dr. D. K. P. Ng by the previously reported route.<sup>8</sup> The compounds were purified by recrystallization from light petroleum (boiling point, 40–60 °C) and subsequent vacuum sublimation. Sample purity was checked by IR, MS, and elemental analysis.

The electronic absorption spectra of the complexes dissolved in *n*-heptane were recorded with a Specord UV–visible (Carl Zeiss, Jena, Germany) instrument in an evacuated quartz cell at room temperature. The construction of the cell made it possible to change the concentration of the complex and to detect both strong and weak absorption bands in a single experiment. The vapor-phase spectra were measured using a heated quartz vacuum cell on the same spectrometer at 80–130 °C. Temperatures were maintained by a coil of resistance wire wrapped around the quartz cell holder.

### Results and Discussion

#### Solution-Phase Electronic Absorption Spectra.

The spectra of (Ch)(Cp)V and (Ch)(Cp')Ta in *n*-heptane solution reveal only broad structureless bands, similar to the solution-phase photoabsorption spectra of the transition-metal sandwiches investigated earlier.<sup>20,21,23–30</sup> The spectrum of (Ch)(Cp)V obtained in this work (Figure 2) agrees well with that reported by Gulick and Geske.<sup>17</sup> It shows an intense peak A, shoulder B, and weak long-wavelength band E. In addition, ill-resolved shoulders C and D are visible which were not revealed in the earlier study.<sup>17</sup> On going to the spectrum of (Ch)(Cp')Ta (Figure 3), the high-frequency structure changes very little, the shoulders C and D appear at lower energies, and two weak but well-defined shoulders E and F are visible instead of the peak E revealed by the (Ch)(Cp)V spectrum. Band frequencies are given in Table 1. The overlapping of absorption bands and absence of vibrational structure make it impossible to interpret unambiguously the solution-phase spectra. However, some assignments are suggested below on the basis of the MO scheme (Figure 1), ligand field (LF) theory,<sup>2,32</sup> simple Huckel MO theory, and PE data<sup>8</sup> after the discussion and assignment of the gas-phase spectra.

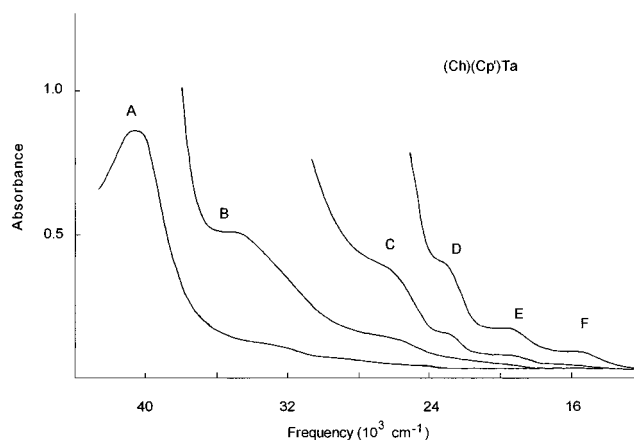


**Figure 3.** Electronic absorption spectrum of (Ch)(Cp')Ta in *n*-heptane solution. Concentrations of (Ch)(Cp')Ta were  $7 \times 10^{-5}$ ,  $3 \times 10^{-4}$ ,  $1 \times 10^{-3}$ , and  $3 \times 10^{-3}$  M.

**Table 1.** Frequencies  $\nu$  ( $\text{cm}^{-1}$ ) of Absorption Bands in Solution-Phase Spectra of (Ch)(Cp)V and (Ch)(Cp')Ta (Figures 2 and 3) and Possible Assignments

compd	band	$\nu$	assignments
(Ch)(Cp)V	A	41 200	Ch( $\pi$ ) $\rightarrow$ Ch( $\delta$ )
	B	36 500	Cp( $\pi$ ) $\rightarrow$ Ch( $\delta$ )
	C	33 000	Cp( $\pi$ ) $\rightarrow$ d( $\pi$ ), Ch( $\pi$ ) $\rightarrow$ d( $\sigma^+$ ), d( $\delta$ ) $\rightarrow$ d( $\pi$ ), d( $\delta$ ) $\rightarrow$ Ch( $\delta$ )
	D	29 500	d( $\sigma^+$ ) $\rightarrow$ d( $\pi$ ), d( $\sigma^+$ ) $\rightarrow$ Ch( $\delta$ )
	E	17 500	Ch( $\pi$ ) $\rightarrow$ Ch( $\delta$ )
(Ch)(Cp')Ta	A	40 500	Ch( $\pi$ ) $\rightarrow$ Ch( $\delta$ )
	B	35 300	Ch( $\pi$ ) $\rightarrow$ d( $\sigma^+$ ), Cp( $\pi$ ) $\rightarrow$ Ch( $\delta$ )
	C	27 100	d( $\delta$ ) $\rightarrow$ Ch( $\delta$ ), Cp( $\pi$ ) $\rightarrow$ d( $\sigma^+$ ), d( $\sigma^+$ ) $\rightarrow$ d( $\pi$ )
	D	23 800	d( $\delta$ ) $\rightarrow$ Ch( $\delta$ ), Cp( $\pi$ ) $\rightarrow$ d( $\sigma^+$ ), d( $\sigma^+$ ) $\rightarrow$ d( $\pi$ )
	E	20 600	d( $\delta$ ) $\rightarrow$ Ch( $\delta$ )
	F	16 800	d( $\delta$ ) $\rightarrow$ d( $\sigma$ )

**Gas-Phase Spectra.** The electronic absorption spectra of (Ch)(Cp)V (Figure 4) and (Ch)(Cp')Ta (Figure 5) in the gas phase are quite different from those recorded in *n*-heptane solution (Figures 2 and 3). In addition to the strong broad peak A observed in the solution phase, they show new absorption bands which were not revealed by the solution spectra. The shoulders B–F (Figures 2 and 3) are unobservable in the vapor-phase spectra because of their low relative intensity. The appearance of new well-defined bands in an electronic absorption spectrum on going from the condensed phase to the vapor phase indicates that corresponding transitions have a Rydberg nature.<sup>22</sup> Indeed, it was demonstrated that all such bands, which are observed in the spectra of the transition-metal sandwich complexes studied earlier,<sup>20,21,23–30</sup> arise from the electronic transitions originating at the nonbonding d( $\sigma^+$ ) orbital and terminating at Rydberg levels. By analogy, the new features appearing in the spectra of gas-phase (Ch)-(Cp)V and (Ch)(Cp')Ta are assigned to Rydberg excitations from MO d( $\sigma^+$ ).

Rydberg transitions in polyatomic molecules are characterized by the term values<sup>22</sup>

$$T = I - \nu = R/(n - \delta)^2 = R/(n^*)^2 \quad (1)$$

where  $I$  is the energy of ionization from the occupied MO participating in the Rydberg excitation,  $\nu$  is the energy of the Rydberg transition,  $R$  is the Rydberg

(31) King, R. B. *Organomet. Synth.* **1965**, *1*, 140.

(32) Ballhausen, C. J. *Introduction to Ligand Field Theory*; McGraw-Hill: New York, 1962.

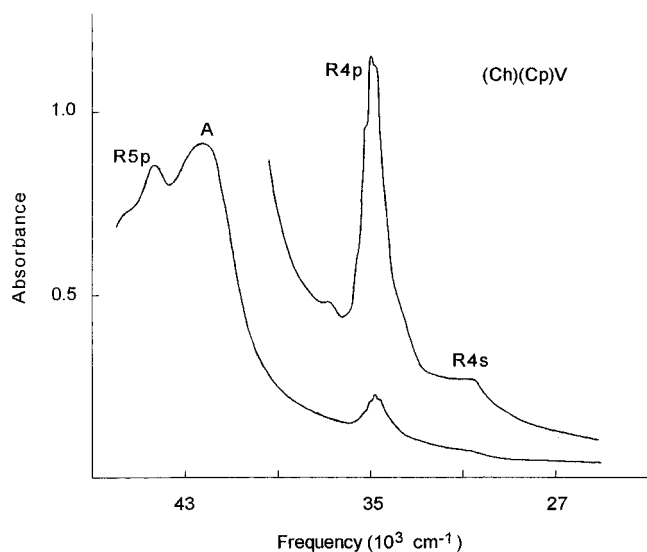


**Figure 4.** Electronic absorption spectrum of (Ch)(Cp)V in the vapor phase.

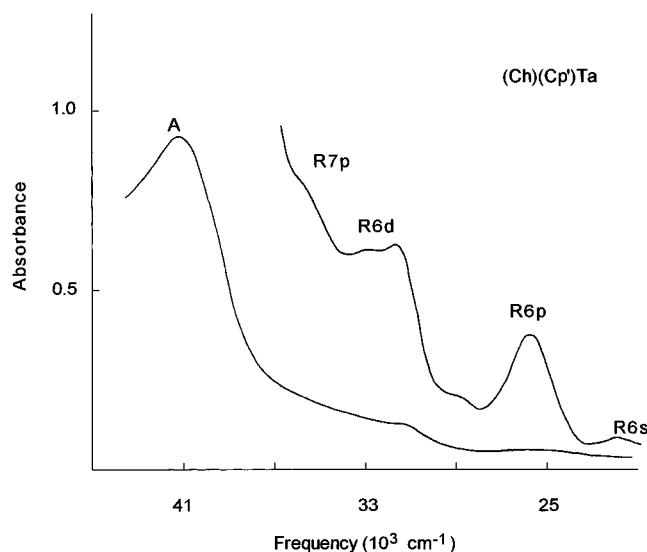


**Figure 5.** Electronic absorption spectrum of (Ch)(Cp)Ta in the vapor phase.

constant ( $109\,737\text{ cm}^{-1}$ ),  $n$  is the principal quantum number,  $\delta$  is the quantum defect, and  $n^*$  represents the effective principal quantum number. Previous studies<sup>20,21,23–30</sup> show that the  $T$  magnitudes of each Rydberg transition in sandwich complexes are very similar. So the term values and, consequently, the effective principal quantum numbers can be used as a rather reliable basis for interpretation of the Rydberg bands in the spectra of gas-phase (Ch)(Cp)V and (Ch)(Cp)Ta. Knowledge of the  $d(\sigma^+)$  IE determined for the titled compounds from the PE spectra<sup>8</sup> (6.49 eV or  $52\,340\text{ cm}^{-1}$  and 5.47 eV or  $44\,120\text{ cm}^{-1}$  for (Ch)(Cp)V and (Ch)(Cp)Ta, respectively) makes it easy to find the parameters of eq 1 for these bands. The  $T$  and  $n^*$  values are presented in Table 2 together with the band frequencies.

The weak shoulder at  $30\,630\text{ cm}^{-1}$  revealed by the (Ch)(Cp)V spectrum has a term value (Table 2) close to that of the lowest Rydberg  $s$  excitation in (Ch)(Cp)Cr<sup>20</sup> ( $21\,390\text{ cm}^{-1}$ ) and (Ch)(Cp)W<sup>21</sup> ( $21\,730\text{ cm}^{-1}$ ). Hence, this shoulder arises from the  $3d(\sigma^+) \rightarrow R4s(\sigma^+)$  transition. The strong peak at  $34\,730\text{ cm}^{-1}$  (Figure 4) is assigned to the  $3d(\sigma^+) \rightarrow R4p(\pi)$  excitation. The term

**Table 2.** Frequencies  $\nu$  ( $\text{cm}^{-1}$ ), Term Values  $T$  ( $\text{cm}^{-1}$ ), Effective Principal Quantum Numbers  $n^*$ , and Assignments of Rydberg Bands in the Electronic Absorption Spectra of Gas-Phase (Ch)(Cp)V and (Ch)(Cp)Ta (Figures 4 and 5)

$\nu$	$T$	$n^*$	assignments <sup>a</sup>
(Ch)(Cp)V			
30 630	21 710	2.25	$3d(\sigma^+) \rightarrow R4s(\sigma^+)$ ( $^2\Sigma^+$ )
34 730	17 610	2.50	$3d(\sigma^+) \rightarrow R4p(\pi)$ ( $^2\Pi$ )
36 650	15 690	2.64	$3d(\sigma^+) \rightarrow R4p(\sigma^+)$ ( $^2\Sigma^+$ )
44 050	8 290	3.64	$3d(\sigma^+) \rightarrow R5p(\pi)$ ( $^2\Pi$ )
45 470	6 870	4.00	$3d(\sigma^+) \rightarrow R5d(\pi)$ ( $^2\Pi$ )
(Ch)(Cp)Ta			
21 900	22 220	2.22	$5d(\sigma^+) \rightarrow R6s(\sigma^+)$ ( $^2\Sigma^+$ )
25 800	18 320	2.49	$5d(\sigma^+) \rightarrow R6p(\pi)$ ( $^2\Pi$ )
28 750	15 370	2.67	$5d(\sigma^+) \rightarrow R6p(\sigma^+)$ ( $^2\Sigma^+$ )
31 500	12 620	2.95	$5d(\sigma^+) \rightarrow R6d(\pi)$ ( $^2\Pi$ )
33 000	11 120	3.14	$5d(\sigma^+) \rightarrow R6d(\delta)$ ( $^2\Delta$ )
35 500	8 620	3.57	$5d(\sigma^+) \rightarrow R7p(\pi)$ ( $^2\Pi$ )

<sup>a</sup> The symmetries of electronic excited states in the  $C_{\infty v}$  point group are given in parentheses.

value corresponding to its maximum coincides with that of the first member of the  $Rmp(\pi)$  series in the vapor-phase spectra of closely related (Ch)(Cp)Cr<sup>20</sup> ( $17\,580\text{ cm}^{-1}$ ), (Bz)<sub>2</sub>V<sup>26</sup> ( $17\,550\text{ cm}^{-1}$ ) (Bz =  $\eta^6\text{-C}_6\text{H}_6$ ) and (Ch)(Cp)Nb<sup>30</sup> ( $17\,610\text{ cm}^{-1}$ ). This peak reveals a  $220\text{ cm}^{-1}$  progression arising from excitations of the totally symmetric metal–ligand stretching vibration in the Rydberg state. A similar separation between the progression members was found for the lowest  $Rmp(\pi)$  transition in other sandwiches with unsubstituted carbocyclic rings.<sup>20,26,28,29</sup>

The weak band at  $36\,650\text{ cm}^{-1}$  (Figure 4) is assigned on the basis of its term value to the  $3d(\sigma^+) \rightarrow R4p(\sigma^+)$  excitation. In the closely related molecules of (Ch)(Cp)Cr, (Bz)<sub>2</sub>V, and (Ch)(Cp)Nb, the lowest Rydberg  $p(\sigma^+)$  transition is characterized by  $T$  values of  $15\,490$ ,  $15\,650$  and  $15\,490\text{ cm}^{-1}$ , respectively.<sup>20,26,30</sup>

The peak at  $44\,050\text{ cm}^{-1}$  in the (Ch)(Cp)V spectrum represents the second member of the  $Rmp(\pi)$  series. Table 2 shows that the corresponding quantum defect ( $\delta = 1.36$ ) is a little lower than that for the first series member ( $\delta = 1.50$ ) as expected from weaker penetration of MO  $R5p(\pi)$  into the molecular core compared with the  $R4p(\pi)$  orbital.<sup>29</sup>

The shoulder at  $45\,470\text{ cm}^{-1}$  (Figure 4) is characterized by the term value and effective principal quantum number appropriate for assigning it as the second member of the  $Rnd$  series. Since the  $Rnd(\pi)$  transitions in the spectra of (Ch)(Cp)Cr and (Ch)(Cp)W are more intense than  $Rnd(\sigma^+)$ ,<sup>20,21</sup> the shoulder considered arises most likely from the  $3d(\sigma^+) \rightarrow R5d(\pi)$  excitation. Thus, all Rydberg features observed in the (Ch)(Cp)V vapor-phase spectrum have been identified in this work.

The intensity distribution in the vibronic structure of the  $R4p(\pi)$  excitation (Figure 4) shows that the 0,0 transition lies two to three vibrational quanta lower than the band maximum. A different picture was observed in the spectra of the 18-electron complexes (Ch)(Cp)Cr,<sup>20</sup> (Bz)<sub>2</sub>Cr,<sup>26</sup> and (Bz)(Cp)Mn,<sup>28,29</sup> where the strongest peak in the vibronic structure of the  $R4p(\pi)$  band corresponds to the 0,0 transition. The difference between the equilibrium metal–ligand distances in the ground and Rydberg state is therefore greater for (Ch)(Cp)V than for the 18-electron sandwiches mentioned above. This may be due to a decrease in the metal character of the (Ch)(Cp)V  $d(\sigma^+)$  orbital or due to an

interaction between the R4p( $\pi$ ) state and valence shell levels in (Ch)(Cp)V. The former effect results in an increase of the metal–ligand distances, which correspond to the minimum on the potential energy surface in each (Ch)(Cp)V Rydberg state and in the (Ch)(Cp)V<sup>+</sup> cation ground electronic state, relative to the equilibrium distances in the ground state of the neutral molecule. In that case, all Rydberg transitions in (Ch)(Cp)V will be broadened, their term values being close to those for 18-electron sandwiches. Supporting evidence for this explanation comes from the observation that the R4s( $\sigma^+$ ), R4p( $\sigma^+$ ), and R5p( $\pi$ ) bands (Figure 4) are also broadened. The spectrum of gas-phase (Ch)(Cp)V shows no narrow Rydberg bands such as those observed in the spectra of (Ch)(Cp)Cr,<sup>20</sup> (Bz)<sub>2</sub>Cr,<sup>26</sup> and (Bz)(Cp)Mn<sup>28,29</sup> while the  $T$  magnitudes for (Ch)(Cp)V (Table 2) coincide with the nonperturbed term values for these closed shell sandwiches within the accuracy given by PE spectroscopy for the d( $\sigma^+$ ) ionization energy (IE) (0.05 eV or  $\sim 400$  cm<sup>-1</sup>).

However, there is at least one Rydberg transition in (Ch)(Cp)V that is broadened predominately by the interaction with an intravalency excitation. That is the first member of the symmetry-allowed Rydberg nd( $\pi$ ) series. In the vapor-phase spectra of 18-electron mixed sandwich complexes<sup>20,21</sup> and (Ch)(Cp)Nb,<sup>30</sup> such a transition is responsible for a strong absorption peak. Its term value is equal to 12 500–12 900 cm<sup>-1</sup>, so the corresponding band should appear in the spectrum of gas phase (Ch)(Cp)V at 39 400–39 800 cm<sup>-1</sup>. However, this spectrum (Figure 4) reveals no absorption features in this frequency range. The 3d( $\sigma^+$ )  $\rightarrow$  R4d( $\pi$ ) transition in (Ch)(Cp)V is therefore broadened beyond detection. Such an effect can be only due to an appreciable admixture of an intravalency excitation.

The Rydberg bands revealed by the (Ch)(Cp')Ta vapor-phase spectrum (Figure 5) are even broader than those in the spectrum of the vanadium complex (Figure 4). As with (Ch)(Cp)V, they can be identified easily on the basis of the corresponding  $T$  and  $n^*$  values. On going from (Ch)(Cp)V to (Ch)(Cp')Ta, the principal quantum number of the metal d<sub>z<sup>2</sup></sub> orbital increases by 2. Consequently, the  $n$  value characterizing each Rydberg orbital undergoes formally the same change. Simultaneously, the quantum defect  $\delta$  should increase also by  $\sim 2$ ,<sup>22</sup> the  $n^*$  value being nearly constant for each Rydberg transition. Indeed, it has been shown that the  $n^*$  and  $T$  magnitudes for Rydberg excitations in sandwich molecules remain very similar on replacing the metal atom with its heavier analogue unless the change is caused by different Rydberg/valence mixing.<sup>20,21,24,27</sup> Accordingly, the parameters of the Rydberg transitions in the (Ch)(Cp')Ta spectrum (Table 2) are close to those for (Ch)(Cp)V and the sandwich complexes studied earlier.<sup>20,21,23–30</sup> Thus an unambiguous interpretation for the Rydberg structure of this spectrum is possible. The band assignments are presented in Table 2.

The introduction of a methyl group into the carbocyclic ring leads usually to a small decrease in the term values of the lowest Rydberg s and p excitations in sandwich molecules.<sup>24,26,29</sup> In contrast, the R6s( $\sigma^+$ ) and R6p( $\pi$ ) term values for (Ch)(Cp')Ta are somewhat larger than the corresponding  $T$  magnitudes for (Ch)(Cp)V (Table 2) and (Ch)(Cp)Nb.<sup>30</sup> This fact is indicative of an interaction between the 5d( $\sigma^+$ )  $\rightarrow$  R6s( $\sigma^+$ ), R6p( $\pi$ )

Rydberg transitions, and higher-lying valence shell excitations in (Ch)(Cp')Ta. The R6p( $\pi$ ) band (Figure 5) can be additionally broadened by the core splitting of the R6p( $\pi$ ) state as a result of symmetry reduction on introduction of the methyl group or by the spin–orbit splitting of this state into the  $E_{1/2}$  and  $E_{3/2}$  components due to the presence of the heavy metal atom.

In contrast to (Ch)(Cp)V, the spectrum of gas-phase (Ch)(Cp')Ta shows two clearly defined peaks corresponding to the lowest Rydberg d transitions. The peak at 31 500 cm<sup>-1</sup> has a term value (Table 2) coinciding with that of the R6d( $\pi$ ) excitation in (Ch)(Cp)W,<sup>21</sup> so it is assigned to the 5d( $\sigma^+$ )  $\rightarrow$  R6d( $\pi$ ) transition. The second R6d band is separated from this peak by 1500 cm<sup>-1</sup> which seems to be too large for the splitting of the R6d( $\pi$ ) state caused by the symmetry reduction or spin–orbit coupling. It seems most likely that the second R6d band is due to the 5d( $\sigma^+$ )  $\rightarrow$  R6d( $\delta$ ) excitation. This transition is symmetry-forbidden for the unsubstituted mixed sandwich complexes, but it becomes allowed if the axial symmetry is broken by the presence of a methyl group in the ring.

The spectrum of (Ch)(Cp')Ta reveals a shoulder at 35 500 cm<sup>-1</sup> arising from the 5d( $\sigma^+$ )  $\rightarrow$  R7p( $\pi$ ) excitation while the higher members of the R $l$ p( $\pi$ ) series are not observed because of their broadening and low intensity. The absence of sharp narrow Rydberg peaks in the (Ch)(Cp')Ta spectrum (Figure 5) suggests that decrease in the metal character of MO 5d( $\sigma^+$ ) combines with the Rydberg/valence mixing to cause broadening of the Rydberg bands.

**Assignment of Solution Spectra.** Ligand field theory remains the most reliable way of assigning d–d transitions. As an empirical method it has the advantage that the parameters deduced for ligands are transferable between complexes, hence the spectrochemical and nephelauxetic series. It has been applied with considerable success to the electronic states of metallocenes.<sup>2</sup>

To estimate the frequencies of such excitations in transition-metal sandwich compounds, a first-order approximation can be used as it was for ( $\eta^6$ -arene)<sub>2</sub>V,<sup>33</sup> ( $\eta^5$ -C<sub>5</sub>Me<sub>5</sub>)<sub>2</sub>Re<sup>+</sup>,<sup>34</sup> and cations of 3d metallocenes.<sup>35</sup> In sandwich molecules with a [d( $\delta$ )]<sup>4</sup> [d( $\sigma^+$ )]<sup>1</sup> ground-state configuration, three d–d promotions are possible which produce four excited electronic states. According to LF theory,<sup>2,32</sup> they are expected to have the following first-order energies:

$$\begin{aligned} d(\delta) \rightarrow d(\sigma^+) & \quad ({}^2\Sigma^+ \rightarrow {}^2\Delta) & \Delta_2 - 20B \\ d(\sigma^+) \rightarrow d(\pi) & \quad ({}^2\Sigma^+ \rightarrow {}^2\Pi) & \Delta_1 + 10B \\ d(\delta) \rightarrow d(\pi) & \quad ({}^2\Sigma^+ \rightarrow {}^2\Pi) & \Delta_1 + \Delta_2 - 4.5B - C \\ & \quad ({}^2\Sigma^+ \rightarrow {}^2\Phi) & \Delta_1 + \Delta_2 - 16.5B - C \quad (2) \end{aligned}$$

where  $\Delta_1$  and  $\Delta_2$  are the LF splittings ( $\epsilon(\pi) - \epsilon(\sigma^+)$  and  $\epsilon(\sigma^+) - \epsilon(\delta)$  respectively) and  $B$  and  $C$  are Racah electron repulsion parameters. The energy of the d( $\delta$ )  $\rightarrow$  d( $\sigma^+$ )

(33) McCamely, A.; Perutz, R. N. *J. Phys. Chem.* **1991**, *95*, 2738.

(34) Bandy, J. A.; Cloke, F. G. N.; Cooper, G.; Day, J. P.; Girling, R. B.; Graham, R. G.; Green, J. C.; Grinter, R.; Perutz, R. N. *J. Am. Chem. Soc.* **1988**, *110*, 5039.

(35) Evans, S.; Green, M. L. H.; Jewitt, B.; King, G. H.; Orchard, A. F. *J. Chem. Soc., Faraday Trans. 2* **1974**, *70*, 356.

**Table 3. Frequencies of Valence Shell Electronic Transitions in (Ch)(Cp)V and (Ch)(Cp')Ta Evaluated on the Basis of Ligand Field Theory, Huckel MO Theory, and P.E. Data**

transition <sup>a</sup>	frequency	
	(Ch)(Cp)V	(Ch)(Cp')Ta
d( $\delta$ ) $\rightarrow$ d( $\sigma^+$ ) <sup>b</sup> ( <sup>2</sup> $\Delta$ )	9 000	16 000
d( $\sigma^+$ ) $\rightarrow$ d( $\pi$ ) <sup>b</sup> ( <sup>2</sup> $\Pi$ ) <sup>g</sup>	20 000	26 000
d( $\delta$ ) $\rightarrow$ d( $\pi$ ) <sup>b</sup> ( <sup>2</sup> $\Pi$ ) <sup>g</sup>	29 000	43 000
d( $\delta$ ) $\rightarrow$ d( $\pi$ ) <sup>b</sup> ( <sup>2</sup> $\Phi$ )	26 000	39 000
Cp( $\pi$ ) $\rightarrow$ Cp( $\delta$ ) ( <sup>2</sup> $\Pi$ <sub>c</sub> + <sup>2</sup> $\Phi$ )	> 50 000	> 50 000
Ch( $\pi$ ) $\rightarrow$ Cp( $\delta$ ) ( <sup>2</sup> $\Pi$ <sub>c</sub> + <sup>2</sup> $\Phi$ )	> 50 000	> 50 000
Ch( $\pi$ ) $\rightarrow$ Ch( $\delta$ ) ( <sup>2</sup> $\Pi$ <sub>c</sub> + <sup>2</sup> $\Phi$ )	41 000	41 000
Cp( $\pi$ ) $\rightarrow$ Ch( $\delta$ ) ( <sup>2</sup> $\Pi$ <sub>c</sub> + <sup>2</sup> $\Phi$ )	29 000	29 000
Ch( $\pi$ ) $\rightarrow$ d( $\sigma^+$ ) ( <sup>2</sup> $\Pi$ ) <sup>e</sup>	27 000	34 000
Cp( $\pi$ ) $\rightarrow$ d( $\sigma^+$ ) ( <sup>2</sup> $\Pi$ ) <sup>e</sup>	13 000	21 000
Ch( $\pi$ ) $\rightarrow$ d( $\pi$ ) ( <sup>2</sup> $\Sigma$ <sup>+</sup> <sub>c</sub> + <sup>2</sup> $\Sigma$ <sup>-</sup> + <sup>2</sup> $\Delta$ )	47 000	60 000
Cp( $\pi$ ) $\rightarrow$ d( $\pi$ ) ( <sup>2</sup> $\Sigma$ <sup>+</sup> <sub>c</sub> + <sup>2</sup> $\Sigma$ <sup>-</sup> + <sup>2</sup> $\Delta$ )	33 000	47 000
d( $\sigma^+$ ) $\rightarrow$ Ch( $\delta$ ) ( <sup>2</sup> $\Delta$ )	14 000	7 000
d( $\sigma^+$ ) $\rightarrow$ Cp( $\delta$ ) ( <sup>2</sup> $\Delta$ )	> 37 000	> 29 000
d( $\delta$ ) $\rightarrow$ Ch( $\delta$ ) ( <sup>2</sup> $\Sigma$ <sup>+</sup> <sub>c</sub> + <sup>2</sup> $\Sigma$ <sup>-</sup> + <sup>2</sup> $\Gamma$ )	23 000	23 000
d( $\delta$ ) $\rightarrow$ Cp( $\delta$ ) ( <sup>2</sup> $\Sigma$ <sup>+</sup> <sub>c</sub> + <sup>2</sup> $\Sigma$ <sup>-</sup> + <sup>2</sup> $\Gamma$ )	> 46 000	> 45 000

<sup>a</sup> The symmetries of the corresponding electronic excited states under the  $C_{5v}$  point group are given in parentheses. <sup>b</sup> The frequencies of d–d transitions were evaluated using eq 2 with the parameters  $\Delta_1 = 17\,000\text{ cm}^{-1}$ ,  $\Delta_2 = 13\,900\text{ cm}^{-1}$ , and  $B = 250\text{ cm}^{-1}$  for (Ch)(Cp)V and  $\Delta_1 = 24\,400\text{ cm}^{-1}$ ,  $\Delta_2 = 19\,900\text{ cm}^{-1}$ , and  $B = 190\text{ cm}^{-1}$  for (Ch)(Cp')Ta. <sup>c</sup> Optically allowed states.

transition in (Ch)(Cp)V and (Ch)(Cp')Ta can be estimated, in a fashion similar to that of bis( $\eta^6$ -arene)-vanadium,<sup>33</sup> from the Racah parameter  $B$  and the LF splitting  $\Delta_2$  deduced for the cations from the PE spectra.<sup>8</sup> To estimate the frequencies of other d–d excitations, it is necessary to know the magnitudes of  $\Delta_1$  and  $C$ . The values of  $\Delta_1$  for the compounds considered are unknown. However, for (Ch)(Cp)V, the  $\Delta_1$  magnitude derived from the electronic absorption spectrum of vanadocene<sup>36,37</sup> ( $\sim 17\,000\text{ cm}^{-1}$ ) can be used since this parameter depends mainly on the interaction between the metal d orbitals and MOs of the Cp ligand.<sup>3–9</sup> Taking the ratio  $C/B \sim 4$ , which is usually accepted for transition-metal complexes,<sup>38</sup> we can predict energies for all d–d transitions in (Ch)(Cp)V. Assuming  $\Delta_1/\Delta_2$  ratios in (Ch)(Cp)V and (Ch)(Cp')Ta to be similar, we find  $\Delta_1$  for the tantalum compound to be  $24\,400\text{ cm}^{-1}$ . Then it becomes possible to estimate the energies of the d–d transitions terminating at the MO d( $\pi$ ) of (Ch)(Cp')Ta. The resulting frequencies are given in Table 3. It should be recognized that a number of simplifying assumptions are made in arriving at these frequencies but they should give a reasonable estimate of the ordering and even the likely magnitude of the transition energies.

The frequency of the d( $\delta$ )  $\rightarrow$  d( $\sigma^+$ ) excitation in (Ch)(Cp)V evaluated in this work ( $\sim 9000\text{ cm}^{-1}$ ) differs considerably from that found on the basis of INDO SCF MO calculations<sup>3</sup> ( $17\,510\text{ cm}^{-1}$ ). However, the energy separation between the <sup>1</sup> $\Sigma^+$  ( $[d(\delta)]^4$ ) and <sup>3</sup> $\Delta$  ( $[d(\delta)]^3$ – $[d(\sigma^+)]^1$ ) states of the (Ch)(Cp)V<sup>+</sup> cation obtained from the INDO calculations ( $37\,100\text{ cm}^{-1}$ ) is much greater than that determined experimentally from the PE spectrum of (Ch)(Cp)V ( $2980\text{ cm}^{-1}$ ).<sup>8</sup> So it is quite possible that the INDO SCF method overestimates the

frequency for the d( $\delta$ )  $\rightarrow$  d( $\sigma^+$ ) transition in (Ch)(Cp)V as well. A very small difference between the IE of the d( $\delta$ ) and d( $\sigma^+$ ) electrons in the vanadium mixed sandwich<sup>8</sup> indicates that the d( $\delta$ )  $\rightarrow$  d( $\sigma^+$ ) excitation should appear in the IR region. This is in accord with the frequency obtained in this work (Table 3). For (Ch)(Cp')Ta, the energy of this transition predicted by LF theory (Table 3) corresponds to the shoulder F (Figure 3).

The frequencies of the d( $\sigma^+$ )  $\rightarrow$  d( $\pi$ ) excitation and the symmetry-allowed component (<sup>2</sup> $\Pi$ ) of the d( $\delta$ )  $\rightarrow$  d( $\pi$ ) transition in (Ch)(Cp)V (Table 3) correlate best with the positions of band E and shoulder D (Figure 2), respectively. Table 3 shows that the d( $\sigma^+$ )  $\rightarrow$  d( $\pi$ ) excitation in (Ch)(Cp')Ta may contribute to the bands C or D and the d( $\delta$ )  $\rightarrow$  d( $\pi$ ) transition to the peak A (Figure 3).

While the energies of d–d promotions can increase significantly between (Ch)(Cp)V and (Ch)(Cp')Ta, the frequencies of intraligand and interligand transitions are expected to be similar in both compounds. Such an assumption is supported by similarity in the IE of the ligand-localized electrons in (Ch)(Cp)V and (Ch)(Cp')Ta.<sup>8</sup> According to simple Huckel MO theory,<sup>39,40</sup> the energy separation between the  $e_1''$  and  $e_2''$  frontier MOs of the cyclopentadienyl group (Figure 1) is  $\sim 6\text{ eV}$ , or  $48\,400\text{ cm}^{-1}$ . Since this separation is increased on mixing with the metal d orbitals (Figure 1), the Cp( $\pi$ )  $\rightarrow$  Cp( $\delta$ ) transition in sandwich complexes should appear in the vacuum UV region. The Ch( $\pi$ )  $\rightarrow$  Cp( $\delta$ ) excitation lies at even higher energies. In the cycloheptatrienyl group, the filled  $e_1''$  MO and singly-occupied  $e_2''$  level are separated<sup>40,41</sup> by  $\sim 34\,000\text{ cm}^{-1}$ . Taking into consideration the increase in the energy separation on going to a sandwich compound (Figure 1), we may conclude that the Ch( $\pi$ )  $\rightarrow$  Ch( $\delta$ ) excitation in the (Ch)(Cp)V and (Ch)(Cp')Ta molecules contributes to peak A (Figures 2 and 3). The energy of this promotion is therefore expected to be  $\sim 41\,000\text{ cm}^{-1}$ . Further justification of this is given below. The value of  $41\,000\text{ cm}^{-1}$  for band A is given as the estimate for this transition energy in Table 2 and is used for subsequent computations of band energies.

Though the energies of electronic transitions in a neutral molecule formally has no relationship with ionization energies, MSX $\alpha$  MO calculations on (Bz)<sub>2</sub>Cr show the difference between the IE of two occupied MOs is very close to that between the energies of electronic excitations from these levels to one and the same ligand-localized vacant MO.<sup>42</sup> It is thus justifiable to use the separation of PE bands as a guide to the possible separation of charge-transfer bands.

The IE of MO Cp( $\pi$ ) in the titled compounds is  $\sim 1.5\text{ eV}$  lower than that of Ch( $\pi$ ). Consequently, the Cp( $\pi$ )  $\rightarrow$  Ch( $\delta$ ) transition should be red shifted from the Ch( $\pi$ )  $\rightarrow$  Ch( $\delta$ ) excitation by  $\sim 12\,000\text{ cm}^{-1}$ . Its frequency would then correspond to the shoulders D and C in the spectra of (Ch)(Cp)V and (Ch)(Cp')Ta, respectively (Table 3).

Among charge-transfer transitions in the compounds considered, there are two excitations terminating at the

(39) Robles, E. S. J.; Ellis, A. M.; Miller, T. A. *J. Phys. Chem.* **1992**, *96*, 8791.

(40) Cotton, F. A. *Chemical Application of Group Theory*; Wiley-Interscience: New York, 1979.

(41) Johnson, R. D. *J. Chem. Phys.* **1991**, *95*, 7108.

(42) Weber, J.; Geoffroy, M.; Goursot, A.; Penigault, E. *J. Am. Chem. Soc.* **1978**, *100*, 3995.

(36) Prins, R.; van Voorst, J. D. W. *J. Chem. Phys.* **1968**, *49*, 4665.

(37) Pavlik, I.; Cerny, V.; Maxova, E. *Collect. Czech. Chem. Commun.* **1972**, *37*, 171.

(38) Sohn, Y. S.; Hendrickson, D. N.; Gray, H. B. *J. Am. Chem. Soc.* **1971**, *93*, 3603.

half-occupied  $d(\sigma^+)$  orbital. The information on IE obtained from PE spectra<sup>8</sup> may be helpful when the frequencies of these excitations are estimated. For  $(Bz)_2V$  ( $Bz = \eta^6-C_6H_6$ ), which is isoelectronic with  $(Ch)-(Cp)V$ , the difference between the  $Bz(\pi_u)$  and  $d(\sigma^+)$  detachment energies<sup>43</sup> is 3.36 eV, or 27 100  $cm^{-1}$ . This value corresponds to the frequency of the  $Bz(\pi_u) \rightarrow d(\sigma^+)$  transition in the  $(Bz)_2V^+$  cation. In the solution-phase spectrum of neutral  $(Bz)_2V$ ,<sup>33</sup> such a transition appears at a frequency  $\sim 5000$   $cm^{-1}$  lower (absorption band maximum at 22 470  $cm^{-1}$ ). Assuming that a similar trend takes place with  $(Ch)(Cp)V$  and  $(Ch)(Cp')Ta$ , it is possible to predict the energies of the  $Ch(\pi) \rightarrow d(\sigma^+)$  and  $Cp(\pi) \rightarrow d(\sigma^+)$  excitations in these molecules. In the PE spectra of  $(Ch)(Cp)V$  and  $(Ch)(Cp')Ta$ ,<sup>8</sup> the bands corresponding to the ionizations from the  $d(\sigma^+)$  and  $Ch(\pi)$  MOs are separated by 31 500 and 38 900  $cm^{-1}$ , respectively. So the  $Ch(\pi) \rightarrow d(\sigma^+)$  transition should appear at  $\sim 27$  000  $cm^{-1}$  in the absorption spectrum of the vanadium complex and at  $\sim 34$  000  $cm^{-1}$  in the spectrum of the tantalum compound. By analogy, we evaluate the energy of the  $Cp(\pi) \rightarrow d(\sigma^+)$  excitation to be  $\sim 13$  000 and  $\sim 21$  000  $cm^{-1}$  for  $(Ch)(Cp)V$  and  $(Ch)(Cp')Ta$ , respectively.

It is seen from Table 3 that the energy of the  $d(\delta) \rightarrow d(\pi)$  transition is close to the sum of the  $d(\delta) \rightarrow d(\sigma^+)$  and  $d(\sigma^+) \rightarrow d(\pi)$  energies. Employing the same principle to other electronic transitions in the molecules considered, it is possible to estimate their frequencies on the basis of the following expressions:

$$\begin{aligned} \nu_{Ch(\pi), Cp(\pi) \rightarrow d(\pi)} &\sim \nu_{Ch(\pi), Cp(\pi) \rightarrow d(\sigma^+)} + \nu_{d(\sigma^+) \rightarrow d(\pi)} \\ \nu_{d(\sigma^+) \rightarrow Ch(\delta), Cp(\delta)} &\sim \nu_{Ch(\pi) \rightarrow Ch(\delta), Cp(\delta)} - \nu_{Ch(\pi) \rightarrow d(\sigma^+)} \\ \nu_{d(\delta) \rightarrow Ch(\delta), Cp(\delta)} &\sim \nu_{d(\delta) \rightarrow d(\sigma^+)} + \nu_{d(\sigma^+) \rightarrow Ch(\delta), Cp(\delta)} \quad (3) \end{aligned}$$

The results are presented in Table 3.

Comparison of the estimated transition energies with the frequencies of absorption bands in the solution spectra of  $(Ch)(Cp)V$  and  $(Ch)(Cp')Ta$  (Table 1) suggests that the intense peak A in both spectra ( $\epsilon = 2.25 \times 10^4$   $L mol^{-1} cm^{-1}$  for  $(Ch)(Cp)V$ <sup>17</sup>) is mainly due to the symmetry-allowed component of the  $Ch(\pi) \rightarrow Ch(\delta)$  excitation. Such an assignment is supported by the presence of a similar peak in the solution-phase spectra of  $(Ch)(Cp)Ti$ ,<sup>18,19</sup>  $(Ch)(Cp)W$ ,<sup>21</sup> and  $(Ch)(Cp)Nb$ .<sup>30</sup> Moreover, the spectrum of  $(Ch)(\eta^5-C_5Me_5)Ti$ <sup>19</sup> reveals only a slight blue shift of this band indicating that, indeed, the peak A arises from the intraligand transition localized on the Ch ligand rather than from an interligand promotion or a charge-transfer excitation involving metal orbitals.

The block of the B–D shoulders in the  $(Ch)(Cp)V$  spectrum (Figure 2) arises from the allowed  $Cp(\pi) \rightarrow d(\pi)$ ,  $Cp(\pi) \rightarrow Ch(\delta)$ ,  $Ch(\pi) \rightarrow d(\sigma^+)$ , and  $d(\delta) \rightarrow d(\pi)$  excitations. The charge-transfer transition  $d(\delta) \rightarrow Ch(\delta)$  can contribute to the red wing of the shoulder D in this block. Band E (Figure 2) is assigned to the  $d(\sigma^+) \rightarrow d(\pi)$  promotion and the symmetry-forbidden  $d(\sigma^+) \rightarrow Ch(\delta)$  excitation. This interpretation is in accord with the low intensity of peak E ( $\epsilon = 32.6$   $L mol^{-1} cm^{-1}$ ),<sup>17</sup> which is close to that of  $d(\sigma^+) \rightarrow d(\pi)$  transition in

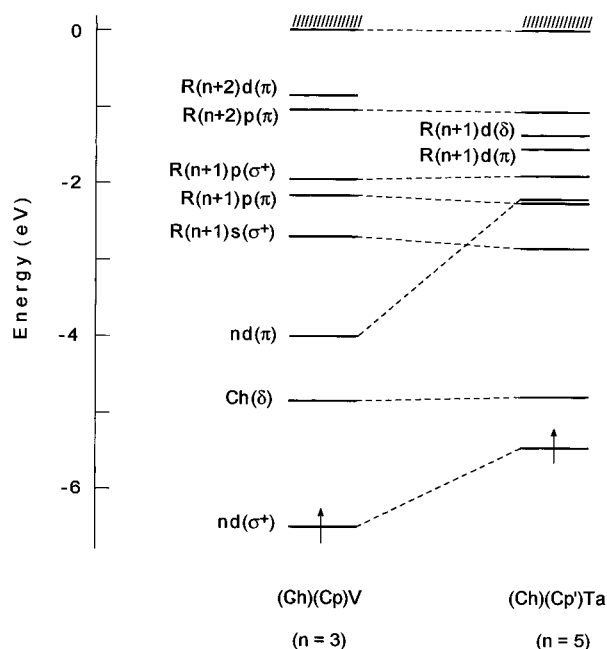


**Figure 6.** IE diagram of vacant levels in the molecules of  $(Ch)(Cp)V$  and  $(Ch)(Cp')Ta$ . The MO positions correspond to the IE determined as the differences between the first IE of the compounds and the frequencies of the electronic transitions originating at the  $d(\sigma^+)$  orbital. The position of the singly-occupied MO  $d(\sigma^+)$  is shown for comparison. The zero level of energy corresponds to the cation ground state.

ferrocene ( $\epsilon = 36$   $L mol^{-1} cm^{-1}$ ).<sup>38</sup> It is unlikely that the allowed  $Cp(\pi) \rightarrow d(\sigma^+)$  excitation, which is expected to give a much more intense band ( $\epsilon = 1800$   $L mol^{-1} cm^{-1}$  for the  $Bz(\pi_u) \rightarrow d(\sigma^+)$  transition in  $(Bz)_2V$ <sup>33</sup>), contributes to peak E in the  $(Ch)(Cp)V$  spectrum though its predicted energy is close to that of  $d(\sigma^+) \rightarrow Ch(\delta)$  (Table 3). This ligand-to-metal transition in the vanadium compound lies most probably in the near-IR region.

On the basis of the estimated frequencies given in Table 3, bands B and C in the spectrum of  $(Ch)(Cp')Ta$  (Figure 3) can be assigned to the  $Ch(\pi) \rightarrow d(\sigma^+)$  and  $Cp(\pi) \rightarrow Ch(\delta)$  excitations. Shoulders D and E in this spectrum may arise from the  $d(\sigma^+) \rightarrow d(\pi)$ ,  $Cp(\pi) \rightarrow d(\sigma^+)$ , and  $d(\delta) \rightarrow Cp(\delta)$  transitions. The longest wavelength band F (Figure 3) corresponds to the symmetry-forbidden  $d(\delta) \rightarrow d(\sigma^+)$  promotion. The proposed assignments of the absorption bands in the solution spectra are summarized in Table 1.

**Ionization Energy Diagram of Vacant Levels.** On the basis of the energies of valence shell excitations evaluated in this work (Table 3) and the parameters of the Rydberg transitions (Table 2), it is possible to determine the order of low-lying states in  $(Ch)(Cp)V$  and  $(Ch)(Cp')Ta$ . The term values of the Rydberg excitations observed are equal to the energies of electron detachment from the Rydberg orbitals in the  $[d(\delta)]^4 [R]^1$  configuration. Since such ionization processes lead to the  $^1\Sigma^+ ([d(\delta)]^4)$  closed shell state of the sandwich cations, they can be adequately described using a one-electron MO approximation. Similarly, the IE of an electron promoted into the valence shell vacant MOs can be calculated as the differences between the  $d(\sigma^+)$  IE and the frequencies of the corresponding intravalency transitions originating at the  $d(\sigma^+)$  orbital.

(43) Cloke, F. G. N.; Dix, A. N.; Green, J. C.; Perutz, R. N.; Seddon, E. A. *Organometallics* **1983**, *2*, 1150.

So we can construct an IE diagram of (Ch)(Cp)V and (Ch)(Cp')Ta empty levels including both Rydberg and valence shell MOs. The scale represents the energy of an ionization process in an excited molecule or the energy of electron attachment to the ground-state cation. This diagram is shown in Figure 6. It is seen that the Rydberg and ligand-localized levels undergo only minor changes on going from (Ch)(Cp)V to (Ch)(Cp')Ta as expected, the main difference being due to the predicted large shift of the  $d(\pi)$  orbital to higher energies. This arises directly from the assumed increase in ligand field splitting on descent of a transition-metal group.

The lowest vacant level in both compounds is formed by the  $\delta$  orbital with dominant cycloheptatrienyl character. Other 17- and 18-electron (Ch)(Cp)M systems are predicted to have the same lowest unfilled MO. Indeed, the ESR study of the 19-electron (Ch)(Cp)Cr<sup>-</sup> anion<sup>10</sup> showed that the unpaired electron in this complex occupies MO Ch( $\delta$ ). The next unoccupied level represents the antibonding  $d(\pi)$  MO in (Ch)(Cp)V and the lowest Rydberg s orbital in (Ch)(Cp')Ta.

### Conclusions

The UV and visible photoabsorption spectra of the gas-phase compounds differ from those recorded in n-pentane solution owing to the presence of Rydberg bands. All Rydberg excitations observed originate at the nonbonding MO  $d(\sigma^+)$ . (Ch)(Cp')Ta represents the first example of the compound with Rydberg transitions from a tantalum-localized orbital. Rydberg bands in the spectra of (Ch)(Cp)V and (Ch)(Cp')Ta are broadened in comparison with those observed in the vapor-phase photoabsorption of (Ch)(Cp)Cr<sup>20</sup> and (Ch)(Cp)W.<sup>21</sup> This may be a result of either decreased metal character of the  $d(\sigma^+)$  MO in the 17-electron (Ch)(Cp)M systems or mixing between Rydberg and valence shell excited states or both factors. The latter effect is revealed in the (Ch)(Cp)V spectrum where the lowest Rydberg  $d(\pi)$  transition is broadened beyond detection due to an admixture of an intravalency excitation. The increased

term values of the  $R6s(\sigma^+)$  and  $R6p(\pi)$  transitions in the spectrum of (Ch)(Cp')Ta are indicative of the Rydberg/valence mixing as well.

The results reported in this work show that the energies of valence shell electronic excitations in the (Ch)(Cp)V and (Ch)(Cp')Ta molecules can be evaluated using ligand field theory,<sup>2,32</sup> Huckel MO theory, and PE data.<sup>8</sup> On the basis of these energies, it is possible to give reasonable qualitative interpretation of the solution-phase UV and visible absorption spectra. The estimated energies of valence shell excitations indicate that electronic transitions can appear in the IR absorption spectra of both complexes.

The IE diagram of vacant levels in (Ch)(Cp)V and (Ch)(Cp')Ta, which has been constructed in this work on the basis of the energies corresponding to the  $[d(\delta)]4$  [vacant MO]1  $\rightarrow$   $[d(\delta)]4$  ionization processes, shows that the Ch( $\delta$ ) level represents the lowest unoccupied MO in both compounds. The lowest Rydberg s and p orbitals fall between the valence shell Ch( $\delta$ ) and Cp( $\delta$ ) vacant MOs. Since the ligand-localized and Rydberg orbitals in sandwich complexes are fairly insensitive to the nature of the central transition metal, this MO order should be retained when vacant levels of other (Ch)(Cp)M systems are described. Thus, the role of Rydberg orbitals must be taken into consideration when analyzing those vapor-phase processes which involve low-lying vacant MOs of transition-metal ( $\eta^7$ -cycloheptatrienyl)-( $\eta^5$ -cyclopentadienyl) derivatives.

**Acknowledgment.** We thank Dr. Sally Jackson and Dr. Dennis Ng for their efforts in synthesizing the sandwich complexes of vanadium and tantalum. We are grateful to the Royal Society for supporting this work. The research described in this publication was made possible in part by Grant N R8F300 from the International Science Foundation and the Russian Government.

OM960137R

(44) Ketkov, S. Yu.; Domrachev, G. A. *Organomet. Chem. U.S.S.R.* **1989**, *2*, 482.